

Research Article

Long-term durability of red mud-modified cement mortars: Effects of high temperature and freeze-thaw cycles

Emrah Turan ^a , Ibrahim A. Alameri ^{b,c,*} , Meral Oltulu ^a

ABSTRACT

The use of industrial by-products such as red mud in cementitious materials addresses sustainability by reducing environmental impact and improving performance. As a hazardous waste from aluminium production, red mud offers a promising solution for waste management and improves the mechanical and durability properties of mortar when used as a partial cement replacement. This study investigates the long-term mechanical and durability properties of cement mortars modified with red mud, a by-product of alumina production. Red mud was incorporated at substitution percentages of 5%, 10%, 15%, 20%, 25%, 30% and 35% by weight of cement. The mortars were subjected to harsh environmental conditions such as high temperatures (200°C to 600°C), freeze-thaw cycles (50 and 100 cycles), and normal curing conditions at 365 days of age. The study showed that partial replacement of cement with red mud significantly affected the mechanical and durability properties of the mortars. The optimum red mud replacement level of 10% showed that microstructural compactness and hardness were improved by increasing the ultrasonic pulse velocity, dynamic modulus of elasticity and flexural strength. Durability tests showed improved thermal resistance at moderate levels of red mud content, while higher levels adversely affected freeze-thaw performance. These findings confirm that a 10% red mud substitution offers the best balance between strength, durability, and sustainability.

ARTICLE INFO

Article history:

Received – January 10, 2025 Revision requested – February 10, 2025 Revision received – March 6, 2025 Accepted – March 20, 2025

Keywords:

Red mud

Waste materials

Physico-mechanical properties

High temperature

Freeze-thaw

SEM-EDX



This is an open access article distributed under the CC BY licence.

© 2025 by the Authors.

Citation: Turan E, Alameri IA, Oltulu M (2025). Long-term durability of red mud-modified cement mortars: Effects of high temperature and freeze-thaw cycles. Challenge Journal of Structural Mechanics, 11(3), 116–127.

1. Introduction

Cement has been increasingly consumed worldwide every year since 1970 (Vedaiyan and Govindarajalu 2023; Verma et al. 2023). Especially in recent years, it has been emphasized that some limitations should be brought in the amount of production and use of cement in terms of both environmental and energy consumption (Alameri and Oltulu 2020; Oltulu and Alameri 2019).

Optimum use of industrial by-products in the concrete (Bergonzoni et al. 2023; Neves et al. 2023), brick (Kostrzewa-Demczuk et al. 2023; Sruthi and Gayathri

2023), tile manufacturing (Pei et al. 2023) and ceramic industries (Liang et al. 2023) reduces the environmental impact of these materials by minimizing the damage from the disposal of residues as well as conserving available resources (Venkatesh et al. 2019, 2020).

Growing social and environmental concerns have driven the increased use of recycled waste materials as partial replacements for natural resources in construction applications (Yavuz 2024; Aboalella and Elmalky 2023). Red mud is a popular industrial waste, which is an alkaline residue (pH value 10–13.5) formed during alumina production. One ton of alumina production usu-

^a Department of Civil Engineering, Atatürk University, Erzurum 25240, Türkiye

^b Department of Civil Engineering, Sana'a University, 13341 Sana'a, Yemen

^c Department of Civil Engineering, Emirates International University, 16881 Sana'a, Yemen

ally yields 0.8 to 1.8 tons of red mud (Hou et al. 2021; Tang et al. 2019). The main recycling method for red clay is landfilling, which pollutes the surrounding soil and groundwater, posing serious threats to human health, food safety and ecosystem sustainability (Hou et al. 2021; Wang et al. 2020).

Red mud is usually discharged as a slurry with a solids content of 15-40% (Yuan et al. 2020). Its chemical and mineralogical composition depends on the source and processing method of bauxite ores, with the main oxides in typical red mud are CaO, SiO₂, Al₂O₃, Fe₂O₃, TiO₂ and Na₂O (Gao et al. 2023; Yuan et al. 2020). Red mud exhibits the properties of porous materials and offers advantages such as high specific surface area, significant reactivity, cost-effectiveness, and significant solid waste utilization potential. Consequently, it can be used as a partial replacement in the production of cement-based materials (Liu et al. 2019).

In the last decade, red mud has been used as a partial substitute of cement and fine aggregates in concrete (Gou et al. 2023; Zhu et al. 2023). The fine particle size of red mud contributes to the densification of the concrete matrix, reducing microcrack formation and increasing durability. Its inclusion reduces workability while increasing both flexural and compressive strength, especially in the later stages of curing. The higher content of red mud-based concretes resulted in a reduction in strength but a lower rate of corrosion (Venkatesh et al. 2019, 2020). Most studies have limited the incorporation of red mud in cement composites to a maximum of 30% (Anirudh et al. 2021; Díaz et al. 2015; Kang and Kwon 2017; Liu et al. 2019; Nikbin et al. 2018; Ortega et al. 2019; Ribeiro et al. 2013; Venkatesh et al. 2019), However, a few researchers have investigated higher replacement levels, exceeding 50% (Krivenko et al. 2017; Tang et al. 2018, 2019; Yuan et al. 2020).

Venkatesh et al. (2019) and Ortega et al. (2019) found that a denser microstructure formation was observed with the red mud substitution and the chloride-ion passage decreased as the red mud substitution increased. Díaz et al. (2015) concluded that additions of red mud delayed both chloride diffusion and carbonation of cement paste samples. Hou et al. (2021) found that the addition of red mud to ultra-high performance concrete reduces workability and mechanical properties while increasing early age (7d) durability due to the accelerated hydration process.

In addition, research has shown that red mud enhances the mechanical properties and durability of cement-based materials. Tang et al. (2019) reported that replacing fly ash with red mud in self-compacting concrete improves strength and corrosion resistance. Yuan et al. (2020) highlighted its micro-filler effect, reducing harmful pores in binary binders. Hyeok-Jung et al. (2018) found it suitable for pavement applications at replacement rates up to 10%, while Li et al. (2019) noted its role in minimizing surface cracks. Tang et al. (2018) observed slight improvements in the interfacial transition zone of red clay concrete.

In contrast to the above studies that emphasized the mechanical performance, durability, and microstructural improvements of red mud in cement-based materi-

als, Nikbin et al. (2018) investigated its environmental impacts. Their research evaluated the sustainability benefits of red mud in concrete, showing that adding 25% red mud to lightweight concrete can significantly reduce environmental impacts, including cumulative energy demand, global warming potential, and emissions of key air pollutants such as CO, NOx, Pb, and SO₂.

Although previous studies have investigated the use of red mud in cement composites, the focus has largely been on its effect on strength and a limited range of durability properties. However, there is a significant gap in understanding its long-term performance, especially under critical environmental conditions. The present study aims to comprehensively investigate the long-term physico-mechanical properties of red mud cement mortars and their durability under freeze-thaw cycles and high-temperature exposure. Moreover, this research provides valuable insights into the applicability of red mud as a sustainable alternative in cement-based materials

2. Materials and Method

2.1. Materials and sample preparation

In this study, ordinary portland cement (CEM II 42.5 R) was used in accordance with TS EN 196-1 (2016) and TS EN 197-1 (2016) standards. Additionally, red mud, characterized by its specific chemical composition and index properties specified in Table 1, was included as a filler material.

Table 1. Chemical composition and index properties of red mud (RM) and portland cement (PC).

		,
Chemical composition (%)	RM	PC
SiO_2	18.95	17.6
Al_2O_3	25.65	4.45
Fe_2O_3	36.94	3.08
CaO	3.30	60.02
MgO	-	2.29
SO_3	-	2.67
Loss on ignition	17.75	8.49
Na ₂ O	7.04	0.22
K ₂ O	-	0.63
Na ₂ O+0.658K ₂ O	-	0.63
Cl	-	0.0144
Unmeasured	-	0.54
Free CaO	-	0.69
Total additives	-	19.9
TiO ₂	5.62	-
Others	2.51	-
index properties		
Specific gravity	3.05	3.01
Specific surface (cm ² /g)	-	4403
Compressive strength (MPa)	-	51.03
рН	12-13	-

The mortar mix design was made according to the TS EN 206 (2014) standard and a water/binder ratio of 0.32 was used. A total of 288 cube specimens (50×50×50 mm) and 32 prism specimens (40×40×160 mm) were prepared, divided into eight groups of cement mortars incorporating red mud at replacement levels of 0%, 5%,

10%, 15%, 20%, 25%, 30%, and 35% by weight of cement. To assess the workability of the fresh concrete, a flow table test was conducted to determine the spreading diameter. Following casting, all samples were cured in water at 25 \pm 2°C for 28 days. Mortar mix proportions are detailed in Table 2.

Table 2. Mortar mix proportions.

Materials used	Cement (%)	Red mud (%)	SPZ (%)	w/b	Spread diameter (cm)
RM0	100	-	0.3	0.32	17.5
RM05	95	5	0.3	0.32	19.5
RM10	90	10	0.3	0.32	17.0
RM15	85	15	0.3	0.32	17.5
RM20	80	20	0.3	0.32	18.0
RM25	75	25	0.3	0.32	17.0
RM30	70	30	0.3	0.32	17.0
RM35	65	35	0.3	0.32	17.0

RM: Red mud, along with its corresponding addition percentage.

SPZ: Superplasticizer.

2.2. Experiments

The impact of reducing cement content through the partial replacement of red mud waste was examined by evaluating the long-term physico-mechanical and durability properties of the specimens. Physico-mechanical properties were assessed based on density, ultrasonic pulse velocity (UPV), dynamic modulus of elasticity (E_d), and compressive strength at 30, 90, and 365 days, as well as flexural strength and modulus of elasticity. Durability performance was analysed by measuring the residual compressive strength after exposure to high temperatures and freeze-thaw cycles.

2.2.1. Density

In this study, the samples were removed from the water pool after 28 days of curing and dried at room conditions (25 °C) for two days. The density of the samples was then calculated by dividing the mass of each sample to the measured volume. The mean value of three samples was calculated for each group to increase the accuracy of the test results.

2.2.2. Ultrasound pulse velocity (UPV)

This test was conducted to evaluate the *UPV* in cement mortar specimens with and without red mud. A digital ultrasonic testing machine operating at 54 kHz was used. Wave propagation time through the mortar samples was determined following the ASTM E494 (2017) standard, and wave velocity was then calculated by dividing the sample length by the recorded time.

The obtained *UPV* was then used to determine the dynamic modulus of elasticity (E_d) using Eq. (1), where ρ represents density, V_{long} denotes longitudinal wave velocity, and ν is Poisson's ratio. In this study, the Poisson's ratio for cement mortars was assumed to be 0.2.

$$E_d = \frac{V_{\text{long}}^2 \cdot \rho \cdot (1+\nu) \cdot (1-2\nu)}{1-\nu} \tag{1}$$

2.2.3. Evaluation of compressive and flexural strength: Testing methods

The compressive and flexural tensile strength tests were carried out following TS EN 12390-3 (2019) and TS EN 12390-6 (2010) standards, respectively, which align with European standards. A 3000 kN capacity testing machine with a position sensor providing 0.001 mm accuracy was used. The load was applied at a constant speed of 0.4 MPa/s for the compressive strength test and 0.04 MPa/s for the flexural tensile strength test. To evaluate the short- and long-term effects of red mud on cement mortar, compression tests were conducted at 30, 90, and 365 days, while flexural strength tests were performed at 365 days. In addition, the modulus of elasticity was determined using the stress-strain curves obtained from 365-day compression tests in accordance with the TS 12390-2 (2019) standard.

2.2.4. High temperature resistance

This study investigated the residual compressive strength of the mortar after exposure to high temperatures. The samples were stored at 25 °C under laboratory conditions and the test was carried out on the 365th day. To prevent explosive spalling caused by steam formation, the samples were pre-dried at 100 °C for 24 h before exposure to high temperatures (Alameri and Oltulu 2020). Heating was carried out in an electric furnace with a maximum capacity of 1000°C following the heating and cooling protocol shown in Fig. 1. The samples were exposed to temperatures of 200 °C, 400 °C, and 600 °C, with a dwell time of 2 hours at each temperature.

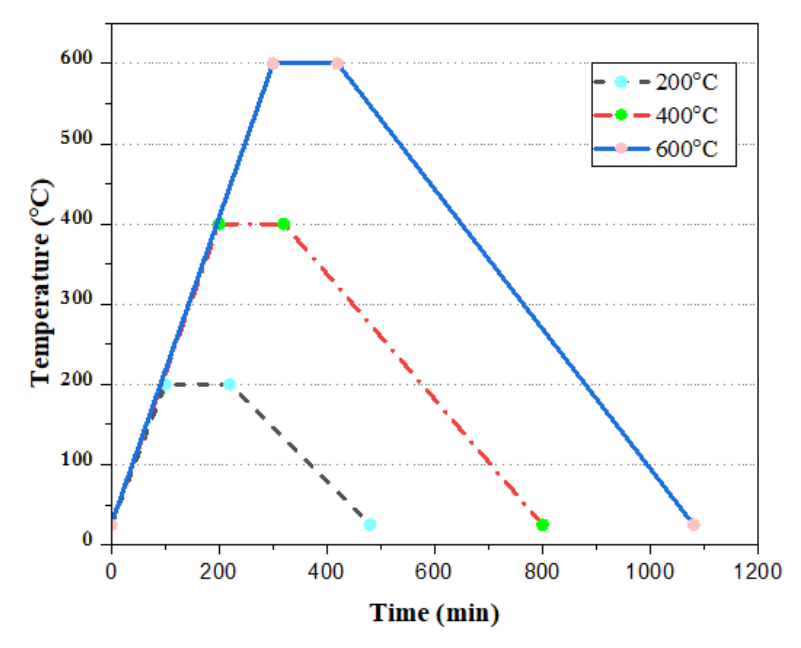


Fig. 1. Heating and cooling regime.

2.2.5. Freeze-thaw resistance

In cold climates such as Erzurum Province, where this experimental study was conducted, cement mortars exposed to freeze-thaw cycles inevitably undergo a certain degree of damage. In this study, 365-day-old cement mortars with and without red mud were subjected to freeze-thaw testing following ASTM C666/C666M (2015) (Procedure A). The samples were subjected to 50 and 100 freeze-thaw cycles, each covering a temperature range of -18 °C to +4 °C for 240 min. After completion of the cycles, the samples were visually inspected and their residual compressive strength was evaluated.

3. Results and Discussion

3.1. Physico-mechanical properties

3.1.1. Density

Density results are summarized in Table 3 and shown in Fig. 2. The density of the mortar mixes showed signif-

icant differences depending on the red mud (RM) content, ranging from 1.96 g/cm³ (RM05) to 2.28 g/cm³ (RM10). Compared to the control mix (RM0) with a density of 1.98 g/cm³, RM10 showed the highest increase, reflecting an increase of 15.15%. This improvement can be attributed to the filler effect of red mud, where the fine particles increased the packing density and contributed to a more compact microstructure. The increased density in RM10 suggests that moderate replacement of cement with red mud increased the overall matrix cohesion, leading to better densification. However, beyond this optimum level, the density showed a downward trend, indicating a decline in structural compactness.

The decrease in density at higher substitution levels, particularly for RM30 ($2.04~g/cm^3$) and RM35 ($2.19~g/cm^3$), indicate an increase in porosity. Excessive red mud content can lead to insufficient cementitious bonding and void formation, which collectively reduces the overall compactness of the mortars.

Table 3.	Physico-mec	hanical	properties.

Group	Density (g/cm³)	UPV (m/s)	E _d (GPa)	30-day compressive strength (MPa)	90-day compressive strength (MPa)	365-day compressive strength (MPa)	Flexural strength (MPa)	E (GPa)
RM0	1.98	3361	20.13	71.01	84.60	87.90	4.93	9.4
RM05	1.96	3252	18.66	76.75	79.10	86.30	5.26	8.6
RM10	2.28	3333	22.80	71.21	75.73	78.70	5.87	8.5
RM15	2.04	3175	18.50	62.31	67.79	72.20	5.76	8.1
RM20	1.98	3200	18.25	58.49	63.40	63.40	5.26	7.5
RM25	2.25	3175	20.41	57.62	60.64	60.70	5.00	7.5
RM30	2.04	3101	17.65	50.85	54.17	61.00	4.73	6.4
RM35	2.19	3175	19.86	46.16	48.75	60.80	4.23	6.5

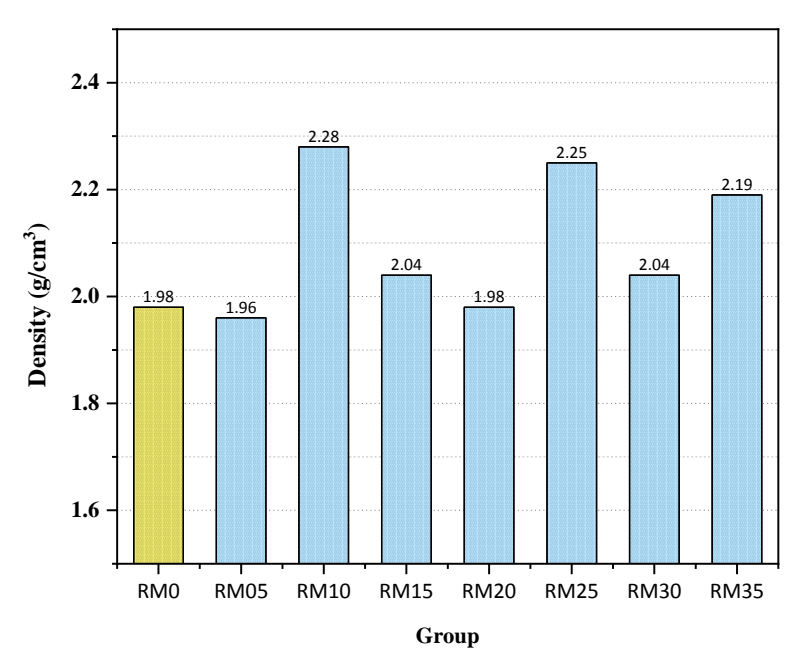


Fig. 2. Density results of the tested groups.

3.1.2. Ultrasonic pulse velocity (UPV)

The UPV results are summarized in Table 3 and shown in Fig. 3. The control group (RM0) showed the highest *UPV* value of 3361 m/s. Among the groups containing red mud, RM10 achieved a *UPV* of 3333 m/s, which was only a 0.83% decrease compared to the control, indicating that up to 10% red mud content did not significantly compromise the density or homogeneity of

the mortar. A consistent decrease in *UPV* was observed with the increase in red mud content, and RM30 showed the lowest speed of 3101 m/s (-7.73%). The observed decrease in *UPV* at higher red clay ratios can be attributed to increased porosity and potential microcrack formation, which hinders wave propagation, as confirmed by other studies linking high additive content to lower pulse speeds due to poor bonding and incomplete hydration (Qureshi et al. 2022).

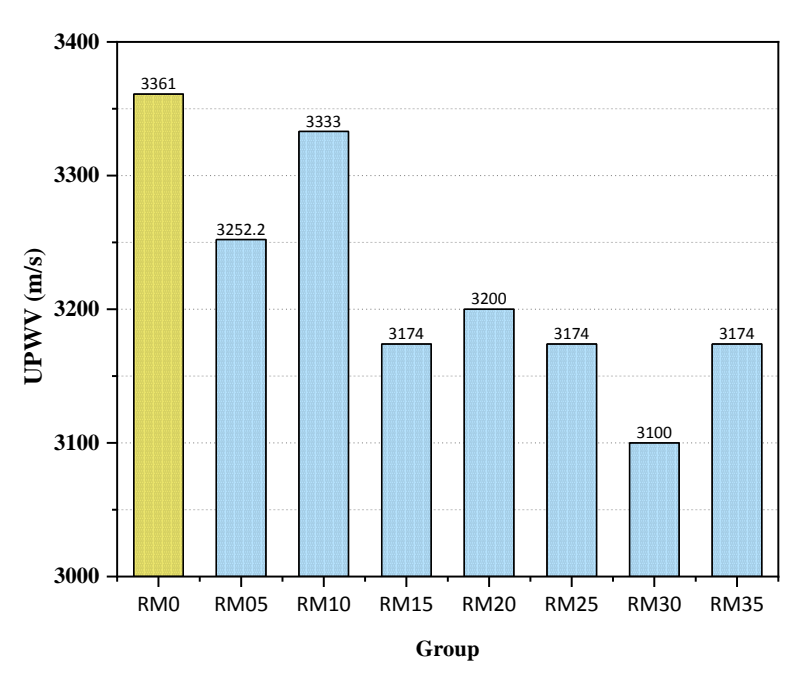


Fig. 3. UPV results of the tested groups.

3.1.3. Dynamic modulus of elasticity (E_d)

The average dynamic modulus of elasticity values of mortars are summarized in Table 3 and shown in Fig. 4.

The dynamic modulus of elasticity (E_d) results showed a strong correlation with both density and ultrasound pulse wave (UPV) velocity, reflecting the stiffness and internal compactness of the mortars. The RM10 group

showed the highest E_d value of 22.80 GPa, representing a 13.2% increase compared to the control group (RM0). RM05 and RM15 showed E_d values of 18.66 GPa and 18.50 GPa, respectively, indicating decreases of approximately 7.3% and 8.0%. Further increases in RM content led to varying effects; RM20 experienced a slight decrease in E_d to 18.25 GPa (-9.5%), while RM25 increased to 20.41 GPa (+1.4%). However, higher RM contents, such as RM30 and RM35, resulted in a decrease in E_d val-

ues of 17.65 GPa (-12.2%) and 19.86 GPa (1.3%), respectively. The variations in E_d values can be attributed to the interplay between UPV and density, both of which affect the E_d . The RM10 group exhibited the highest UPV, which, together with its optimal density, contributed to its superior E_d value. Adding red mud up to a 10% replacement ratio appears to optimize these properties, increasing the stiffness and structural performance of the material.

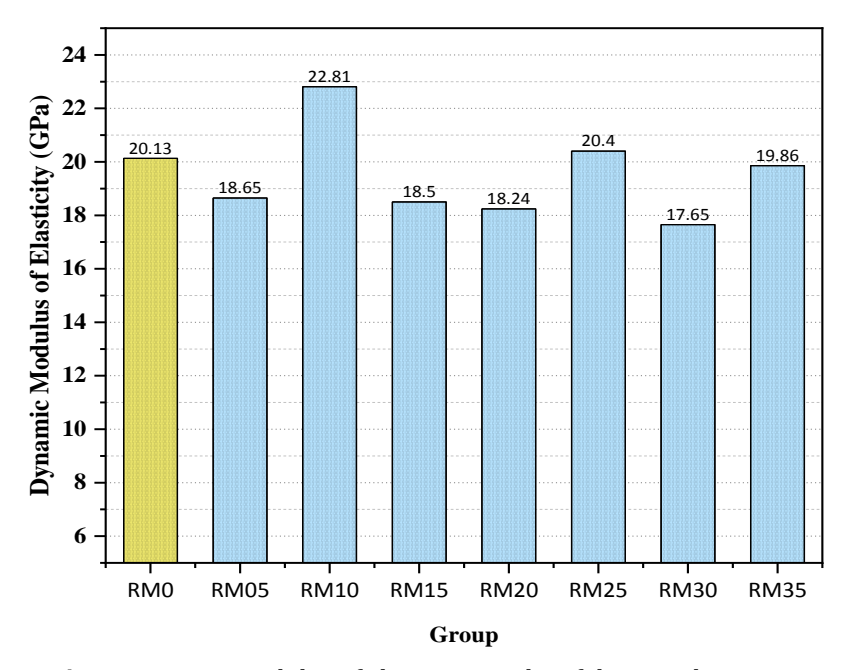


Fig. 4. Dynamic modulus of elasticity results of the tested groups.

3.1.4. Compressive strength

The compressive strength results at different ages showed significant variations depending on the red mud (RM) content (Table 3 and Fig. 5). At 30 days, the RM05 group achieved the highest compressive strength of 76.75 MPa, surpassing the control group (RM0) by approximately 8.1%. This improvement is primarily attributed to the filler effect of the red mud particles, which occupy voids within the cement matrix, leading to a denser microstructure and improved early-age strength. Additionally, the pozzolanic activity of the red mud contributes to the formation of calcium silicate hydrate (C-S-H) gel, further increasing the strength. However, a gradual decrease in compressive strength was observed as the red mud content increased beyond 5%. The RM15 group showed a decrease to 62.31 MPa (-12.3%). This decrease can be attributed to several factors, including that excessive RM can reduce strength by increasing total porosity. Replacing cement with RM reduces the overall amount of cementitious material, potentially weakening the bond strength between the cement paste and the aggregates (Ai et al. 2021; Wang and Zhen 2024).

At 90 days, the control group (RM0) showed the largest increase in compressive strength, increasing by approximately 19.1%, from 71.01 MPa at 28 days to 84.60 MPa at 90 days. This improvement is due to the continuous hydration of the cement particles, which allows the

matrix to gain strength over time. In contrast, groups with red mud content showed more modest increases in strength or relatively smaller changes. Compared to 30day strength, the RM05 group increased (+3.0%), RM10 (+6.3%), RM15 (+8.8%), RM20 (+8.5%), RM25 (+5.2%), RM30 (+6.3%), and RM35 (+5.5%). These results suggest that the incorporation of red mud (up to 20%) leads to an increase in compressive strength at 90 days compared to the 28-day strength. However, when the red mud content exceeds 20%, the strength gain begins to decrease. Adding up to 20% red mud to cementitious materials increases compressive strength gain over time, which is attributed to its pozzolanic activity that contributes to cement hydration and forms additional C-S-H gel, improving the microstructure and strength of the mortar. Beyond this threshold, the introduction of impurities such as sodium, iron, and other alkaline compounds can interfere with the hydration process, inhibiting C-S-H gel formation and weakening the bond between cement particles and aggregates. In addition, higher red mud content can increase porosity, resulting in a less dense microstructure and reduced strength.

At 365 days, the control group (RM0) exhibits a strength increase of approximately 3.9%, rising from 84.60 MPa at 90 days to 87.90 MPa at 365 days. Similarly, the RM10 group shows a 3.92% increase, with strengths increasing from 75.73 MPa at 90 days to 78.70 MPa at 365 days. In contrast, the RM35 group experiences a

more substantial gain of 24.72%, with compressive strength increasing from 48.75 MPa at 90 days to 60.80 MPa at 365 days. These observations suggest that higher

red mud content may contribute to long-term strength development, potentially due to ongoing pozzolanic reactions and microstructural improvements over time.

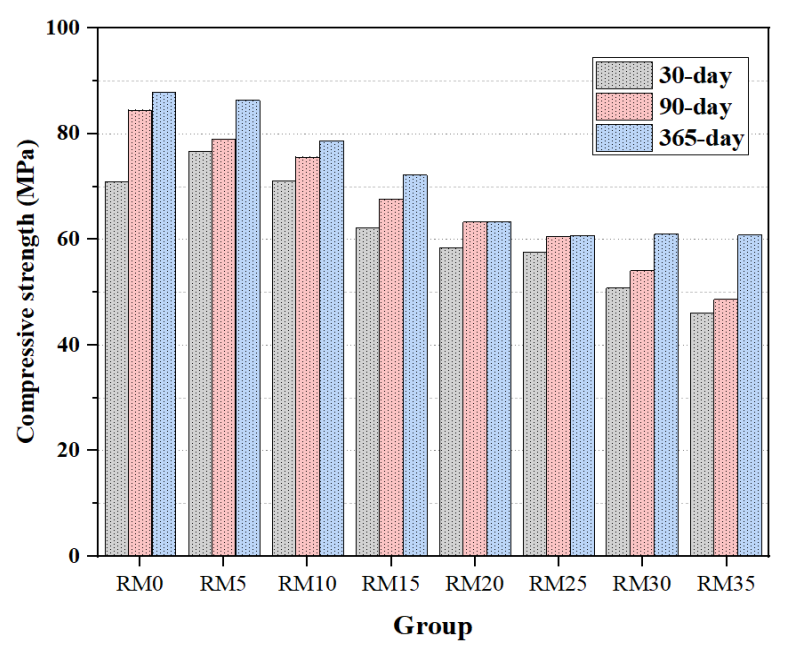


Fig. 5. 30-day, 90-day and 365-day compressive strength results.

As shown in the stress-strain curve (Fig. 6), the stress-strain response in red mud-containing mortars remained more stable beyond the ultimate strength, while the reference group (RM0) showed a sharp decrease.

This behaviour may be due to the densification effect of red mud at optimal levels, which enhances post-peak structural integrity by improving the pore structure and load redistribution mechanisms.

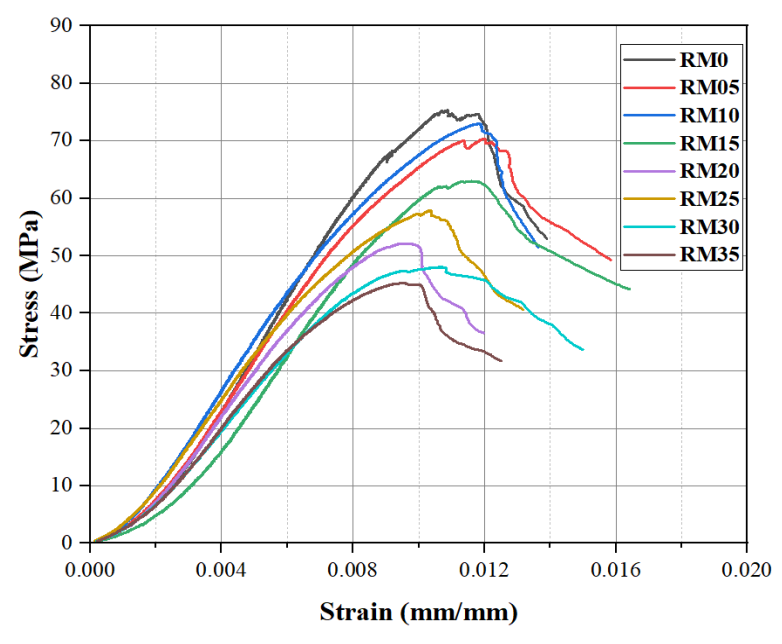


Fig. 6. 28-day stress-strain curves.

3.1.5. Modulus of elasticity

The modulus of elasticity (*E*) results are summarized in Table 3 and shown in Fig. 7. The results showed a clear dependence on the red mud (RM) content, reflecting the changes in stiffness and material deformation

behaviour. The RM0 (control) group exhibits the highest *E* at 9.4 GPa. The RM05 group shows a decrease of approximately 8.51% compared to the control. The modulus of elasticity continues to decrease as the red mud content increases, with the RM30 group experiencing a significant decrease of approximately 31.91%. The

RM35 group also shows a significant decrease in E of approximately 30.85% compared to the control. The decrease in E can be attributed to the deterioration of the

uniformity and compactness of the microstructure, resulting in a less rigid network and hence a lower modulus

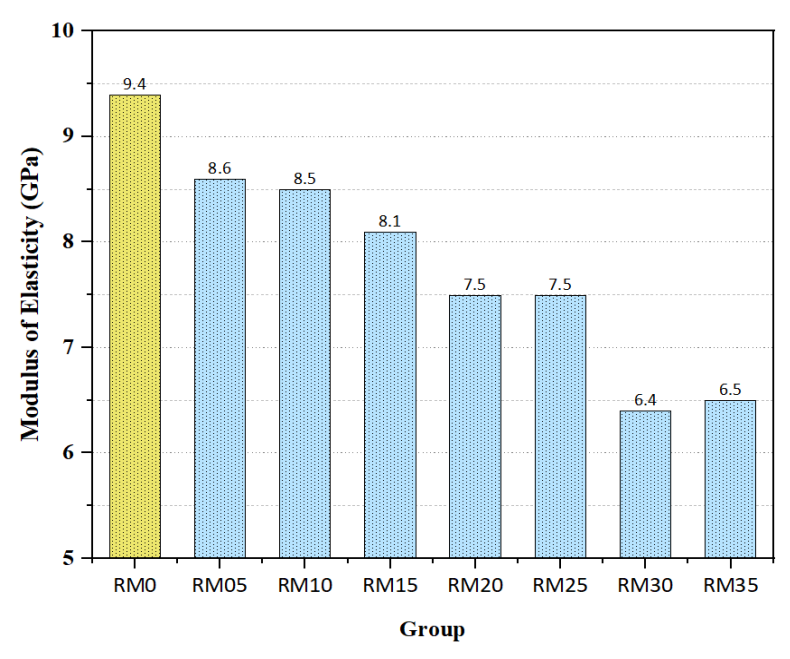


Fig. 7. Modulus of elasticity results of the tested groups.

3.1.6. Flexural tensile strength

In this study, the long term (365-day) flexural tensile strength was examined and the results are summarized in Table 3 and shown in Fig. 8. This improvement in flexural strength continues up to the 10% replacement level, after which strength begins to decrease. The RM10 group exhibits the highest flexural strength at 5.87 MPa, an increase of approximately 19.1% compared to the control group. The RM15 group exhibits a slight decrease to 5.76 MPa (approximately 16.8% higher than the control group), and the RM35 group exhibits the low-

est flexural strength at 4.23 MPa, a decrease of approximately 14.2% compared to the control group. A similar trend was observed for compressive strength, where excessive red mud resulted in reduced strength due to increased porosity and weaker cementitious bonding. This correlation indicates that beyond 10% red mud content, red mud impairs matrix integrity, adversely affecting both tensile and compressive performance. These findings confirm that moderate red mud inclusion enhances strength, while excessive amounts negatively affect the mechanical properties, highlighting the importance of optimized replacement levels for structural reliability.

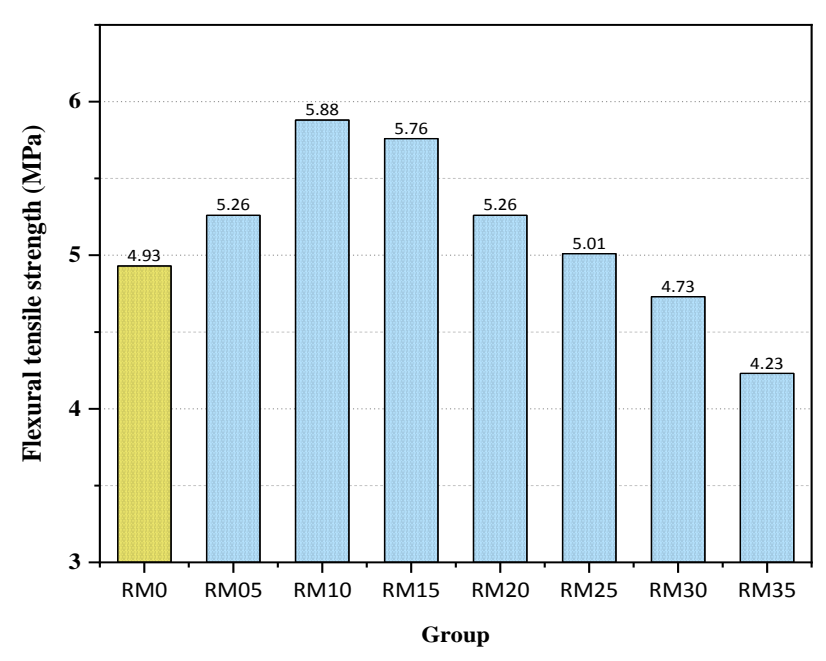


Fig. 8. Flexural strength results of the tested groups.

3.1.7. Durability properties

3.1.7.a. Effect of exposure temperature on compressive strength

Residual compressive strength results are summarized in Table 4 and shown in Fig. 9. After 365 days of normal curing, the control mixture (RM0) exhibited a compressive strength of 87.9 MPa, which increased to 95.5 MPa, reflecting an 8.6% strength gain after exposure to 200°C. This improvement is attributed to the continuous hydration of unreacted cement particles and the reduction of free water, which increases matrix densification. Similarly, RM15 and RM20 showed the highest strength increases, rising by 10.2% and 13.9%, respectively.

In contrast, RM10 and RM05 showed reductions of 8.9% and 7.5%, respectively, indicating that certain RM levels may cause internal shrinkage stresses or increased microcracks under thermal exposure. Although RM15 and RM20 outperformed RM0 in relative strength gain, higher RM contents exhibited decreasing thermal efficiency. RM30 and RM35 only retained 65.5 MPa and 62.0 MPa, respectively, which are 31.4% and 35.1% lower than RM0 at 200°C. Although these groups showed minor strength improvements compared to their normal case values (7.4% and 2.0%, respectively), their overall performance remained significantly weaker than the control. This suggests that excessive RM replacement increased porosity and weakened cementitious bonding, leading to lower thermal resistance.

At 400 °C, the control group (RM0) experienced a significant strength reduction, decreasing from 87.9 MPa to 68.7 MPa (21.9% reduction), indicating thermal-induced microcracking and dehydration effects. RM05, RM10, and RM15 showed similar reductions of 22.8%, 14.1%, and 13.5%, respectively, indicating that moderate RM incorporation slightly improved the thermal resistance. However, higher RM contents (RM20–RM35) experienced larger reductions, with RM35 decreasing by 30.6%.

Compared with RM0 at 400 °C, RM10 and RM15 retained higher strength (67.6 MPa and 62.4 MPa, respec-

tively) with less than 15% loss, indicating improved thermal stability. However, RM30 and RM35 exhibited 17.0% and 38.7% lower strength than RM0, respectively, confirming that excessive RM incorporation leads to thermal degradation.

After exposure to 600 °C, the control mix (RM0) experienced a significant strength reduction, from 87.9 MPa to 62.9 MPa, representing a 28.5% loss. RM05 and RM10 showed a strength reduction of 35.1% and 32.8%, respectively. Although moderate red mud incorporation slightly alleviated thermal degradation, strength losses remained significant. In contrast, RM15 showed a slight strength increase of 3.9%.

3.1.7.b. Effect of freeze-thaw on compressive strength

Residual compressive strength results are summarized in Table 4 and shown in Fig. 10. After 50 freezethaw cycles, the control group (RM0) showed a decrease in compressive strength from 87.9 MPa to 81.6 MPa, a decrease of 6.3%, indicating the effect of freeze-thaw cycles on the cementitious matrix, leading to microcracks and pore expansion. RM05, RM10, RM15, RM20, and RM25 showed similar decreases of 12.4%, 17.6%, 16.2%, 26.4%, and 14.5%, respectively, indicating that RM incorporation experienced more significant strength losses due to freeze-thaw damage by weakening the microstructure and increasing water absorption during the cycles.

After 100 freeze-thaw cycles, the control group (RM0) deteriorated further and decreased to 76.0 MPa (13.5% decrease from the original 87.9 MPa). This decrease is attributed to extensive internal damage due to repeated freezing and thawing, which increased pore connectivity and promoted cracking. Similarly, RM05, RM10, and RM15 showed decreases of 14.9%, 15.2%, and 30.2%, respectively. In particular, RM30 and RM35 showed larger decreases of 39.5% and 40.0%; indicating that higher red mud contents significantly reduce freeze-thaw durability, probably due to weaker microstructural cohesion and increased porosity.

Table 4. Compressive strength test results after exposure to high temperatures and freeze-thaw cy	cles.
--	-------

Croun	365-day avg. comp. strength after high temp. (MPa)			365-day avg. comp. after freeze thaw cycles (MPa)	
Group –	200°C	400°C	600°C	50 cycles	100 cycles
RM0	95.5	68.7	62.9	81.6	76.0
RM5	79.8	66.6	56.1	75.5	73.5
RM10	71.7	67.6	53.3	61.9	50.0
RM15	79.6	62.4	65.0	60.5	50.1
RM20	72.2	52.4	52.4	43.6	41.0
RM25	65.9	61.4	44.0	52.0	47.9
RM30	65.5	57.0	50.0	43.3	37.0
RM35	62.0	42.1	46.1	44.4	36.0

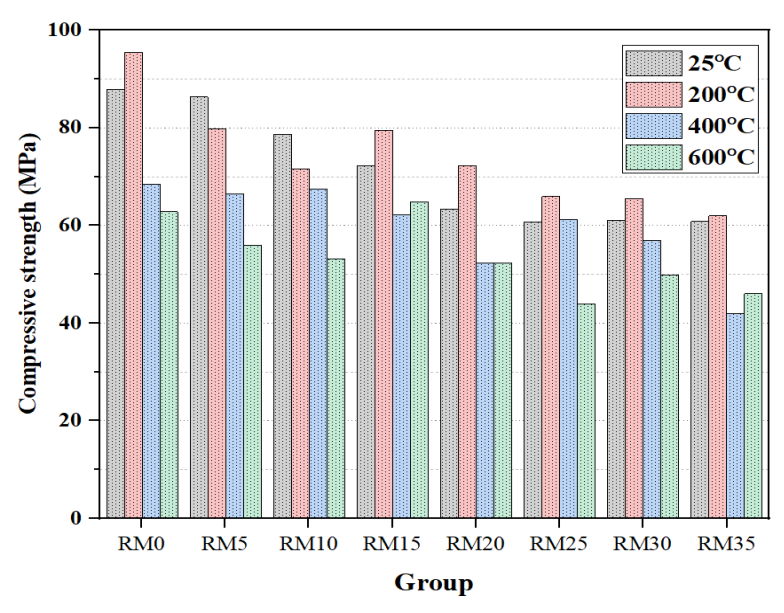


Fig. 9. 365-day average compressive strength results of the tested groups after exposure to elevated temperatures.

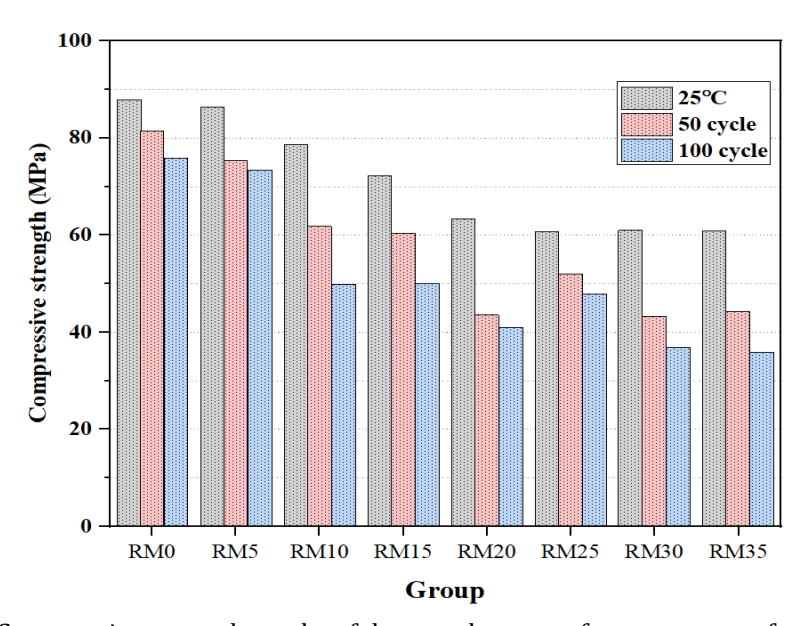


Fig. 10. Compressive strength results of the tested groups after exposure to freeze-thaw.

SEM-EDX analysis was conducted on sample RM5 to examine its microstructure and confirm the uniform distribution of red mud. Additionally, EDX results revealed the chemical composition present in the sample (Fig. 11).

4. Conclusions

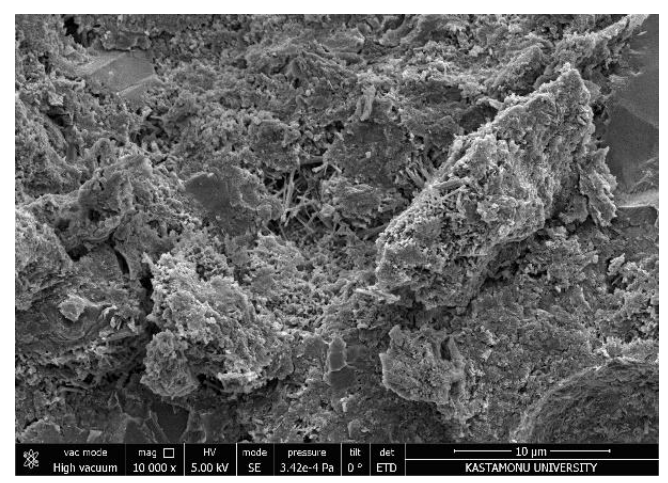
This study investigated the effects of red mud (RM) incorporation on the mechanical properties of cement mortars, with particular emphasis on compressive strength, durability under thermal and freeze-thaw conditions, and long-term effects after 365 days. The results revealed that:

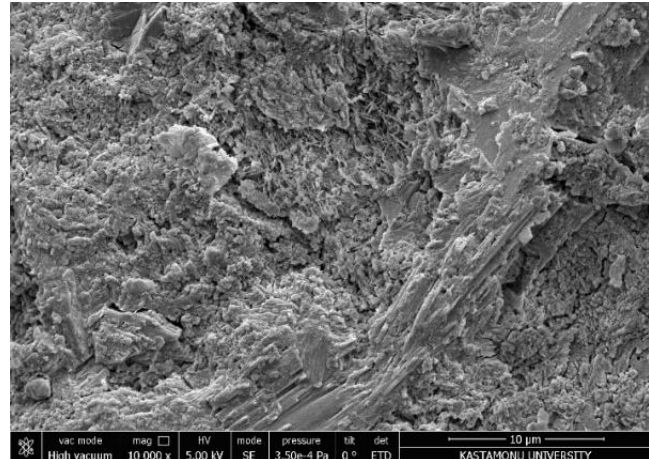
Incorporating red mud at a 10% replacement ratio provided optimal enhancement of mortar performance, significantly improving density, dynamic modulus of elasticity, and flexural strength due to better particle packing and refined microstructural compactness.

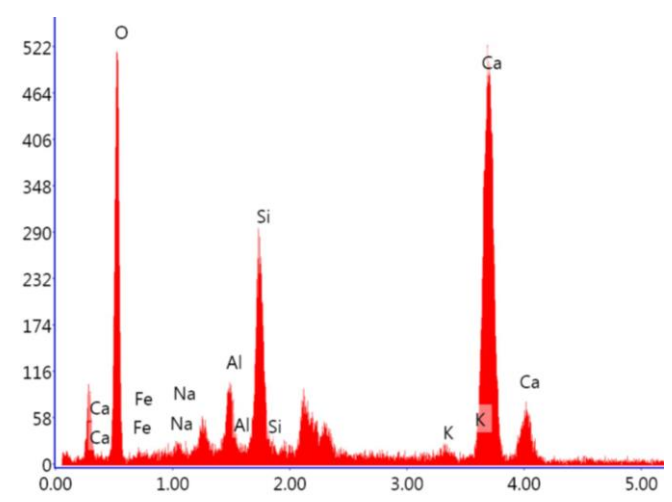
- Compressive strength results showed that red mud content up to 10% increased early and long-term strength, while higher replacement levels (above 20%) led to strength reduction due to increased porosity and decreased cementitious bonding.
- Durability assessments revealed that moderate red mud incorporation improved thermal resistance up to 400 °C, while higher contents significantly reduced freeze-thaw resistance, primarily due to poor microstructural integrity.

The following recommendations are provided for future studies:

- Examination of the changes in properties with different curing methods.
- Detailed pore structure and microstructural studies are recommended on the subject.
- Examination the other durability properties such as acidic and sulphate attack.







Element	Weight (%)	Atomic (%)
0	47.3	67.54
Na	0.72	0.71
Al	2.42	2.05
Si	7.48	6.09
K	0.61	0.36
Ca	39.08	22.27
Fe	2.40	0.98

Fig. 11. SEM-EDX analysis of sample RM5.

Acknowledgements

None declared.

Funding

The authors received no financial support for the research, authorship, and/or publication of this manuscript.

Conflict of Interest

The authors declared no potential conflicts of interest with respect to the research, authorship, and/or publication of this manuscript.

Author Contributions

All of the authors made substantial contributions to conception and design, or acquisition of data, or analysis and interpretation of data; were involved in drafting the manuscript or revising it critically for important intellectual content; and gave final approval of the version to be published.

Data Availability

The datasets created and/or analyzed during the current study are not publicly available, but are available from the corresponding author upon reasonable request.

REFERENCES

Aboalella AA, Elmalky A (2023). Use of crushed bricks and recycled concrete as replacement for fine and coarse aggregates for sustainable concrete production. *Challenge Journal of Concrete Research Letters*, 14(2), 39-46.

Ai T, Zhong D, Zhang Y, Zong J, Yan X, Niu Y (2021). The effect of red mud content on the compressive strength of geopolymers under different curing systems. *Buildings*, 11(7), 298.

Alameri IA, Oltulu M (2020). The physico-mechanical properties of concrete with red mud at high temperatures. *Challenge Journal of Concrete Research Letters*, 11(4), 82-91.

Anirudh M, Rekha KS, Venkatesh C, Nerella R (2021). Characterization of red mud based cement mortar; mechanical and microstructure studies. *Materials Today: Proceedings*, 43, 1587-1591.

ASTM C666 / C666M - 15 (2015). Standard test method for resistance of concrete to rapid freezing and thawing. ASTM International, West Conshohocken, PA, USA.

ASTM E494 – 95 (2017). Standard practice for measuring ultrasonic velocity in materials. ASTM International, West Conshohocken, PA, USA.

Bergonzoni M, Melloni R, Botti L (2023). Analysis of sustainable concrete obtained from the by-products of an industrial process and recycled aggregates from construction and demolition waste. *Procedia Computer Science*, 217, 41-51.

Díaz B, Freire L, Nóvoa XR, Pérez MC (2015). Chloride and $\rm CO_2$ transport in cement paste containing red mud. Cement and Concrete Composites, 62, 178-186.

- Gao Y, Li Z, Xin G, Shen Q, Zhang J, Yang Y (2023). Utilization of highvolume red mud application in cement-based grouting material: Effects on mechanical properties at different activation modes. *Jour*nal of Materials in Civil Engineering, 35(4), 04023011.
- Gou M, Hou W, Zhou L, Zhao J, Zhao M (2023). Preparation and properties of calcium aluminate cement with Bayer red mud. Construction and Building Materials, 373, 130827.
- Hou D, Wu D, Wang X, Gao S, Yu R, Li M, Wang P, Wang Y (2021). Sustainable use of red mud in ultra-high performance concrete (UHPC): Design and performance evaluation. *Cement and Concrete Composites*. 115, 103862.
- Hyeok-Jung K, Kang SP, Choe GC (2018). Effect of red mud content on strength and efflorescence in pavement using alkali-activated slag cement. *International Journal of Concrete Structures and Materials*, 12, 19
- Kang SP, Kwon SJ (2017). Effects of red mud and alkali-activated slag cement on efflorescence in cement mortar. Construction and Building Materials, 133, 459-467.
- Kostrzewa-Demczuk P, Stepien A, Dachowski R, da Silva RB (2023). Influence of waste basalt powder addition on the microstructure and mechanical properties of autoclave brick. *Materials*, 16(2), 870.
- Krivenko P, Kovalchuk O, Pasko A, Croymans T, Hult M, Lutter G, Vandevenne N, Schreurs S, Schroeyers W (2017). Development of alkali activated cements and concrete mixture design with high volumes of red mud. Construction and Building Materials, 151, 819-826.
- Li X, Zhang Q, Mao S, Li L, Wang J (2019). Study on the preparation and fracture behavior of red mud-yellow phosphorus slag-based concrete. *Advances in Materials Science and Engineering*, 2019, 1-15.
- Liang L, Du X, Gao X, Wang Y, Zhang J, Xue X, Shi S, Su N, Zhang K, Li G (2023). Construction and optimization of Fe₃O₄/C/ceramic composite absorbents by one-step recycling red mud and coal hydrogasification residue. *Materials Today Communications*, 34, 105303.
- Liu C, Wu H, Jiang J, Wang L, Kong D, Yu K (2023). Properties of flue gas desulphurization gypsum-activated steel slag fine aggregate red mud-based concrete. *Journal of Materials in Civil Engineering*, 35(4), 04023025.
- Liu Z, Zhang S, Hu D, Zhang Y, Lv H, Liu C, Chen Y, Sun J (2019). Paraffin/red mud phase change energy storage composite incorporated gypsum-based and cement-based materials: Microstructures, thermal and mechanical properties. *Journal of Hazardous Materials*, 364, 608-620.
- Neves A, Almeida J, Cruz F, Miranda T, Cunha VMCF, Rodrigues M, Costa J, Pereira EB (2023). Design procedures for sustainable structural concretes using wastes and industrial by-products. *Applied Sciences*, 13(4), 2087.
- Nikbin IM, Aliaghazadeh M, Charkhtab S, Fathollahpour A (2018). Environmental impacts and mechanical properties of lightweight concrete containing bauxite residue (red mud). *Journal of Cleaner Production*, 172, 2683-2694.
- Oltulu M, Alameri I (2019). The mechanical properties of concrete with red mud (bauxite residue) and nano-Al $_2$ O $_3$ at high temperatures. Fresenius Environmental Bulletin, 28(6), 4692-4701.
- Ortega J, Cabeza M, Tenza-Abril A, Real-Herraiz T, Climent M, Sánchez I (2019). Effects of red mud addition in the microstructure, durability and mechanical performance of cement mortars. *Applied Sciences*, 9(5), 984.
- Pei J, Pan X, Wang Y, Lv Z, Yu H, Tu G (2023). Effects of alkali and alkaline-earth oxides on preparation of red mud based ultra-light-weight ceramsite. *Ceramics International*, 49(11, Part B), 18379-18387

- Qureshi HJ, Ahmad J, Majdi A, Saleem MU, Al Fuhaid AF, Arifuzzaman M (2022). A study on sustainable concrete with partial substitution of cement with red mud: A review. *Materials*, 15(21), 7761.
- Ribeiro DV, Silva AS, Labrincha JA, Morelli MR (2013). Rheological properties and hydration behavior of portland cement mortars containing calcined red mud. *Canadian Journal of Civil Engineering*, 40(6), 557-566.
- Sruthi S, Gayathri V (2023). Synthesis and evaluation of eco-friendly, ambient-cured, geopolymer-based bricks using industrial by-products. *Buildings*, 13(2), 510.
- Tang WC, Wang Z, Liu Y, Cui HZ (2018). Influence of red mud on fresh and hardened properties of self-compacting concrete. *Construction and Building Materials*, 178, 288-300.
- Tang WC, Wang Z, Donne SW, Forghani M, Liu Y (2019). Influence of red mud on mechanical and durability performance of self-compacting concrete. *Journal of Hazardous Materials*, 379, 120802.
- TS EN 196-1 (2016). Methods of testing cement Part 1: Determination of strength. Turkish Standards Institution, Ankara, Türkiye.
- TS EN 197-1 (2016). Cement Composition, specifications and conformity criteria for common cements. Turkish Standards Institution, Ankara, Türkiye.
- TS EN 206 (2014). Concrete Specification, performance, production, and conformity. Turkish Standards Institution, Ankara, Türkiye.
- TS EN 12390-3 (2019). Testing hardened concrete Part 3: Compressive strength of test specimens. Turkish Standards Institution, Ankara, Türkiye.
- TS EN 12390-6 (2010). Testing hardened concrete Part 6: Tensile splitting strength of test specimens. Turkish Standards Institution, Ankara, Türkiye.
- Vedaiyan B, Govindarajalu E (2023). A multi-objective robust grey wolf optimization model for the study of concrete mix using copper slag and glass powder. *International Journal of Advanced Manufacturing Technology*, 125(3), 1941-1953.
- Venkatesh C, Nerella R, Chand MSR (2019). Comparison of mechanical and durability properties of treated and untreated red mud concrete. *Materials Today: Proceedings*, 27, 284-287.
- Venkatesh C, Nerella R, Chand MSR (2020). Experimental investigation of strength, durability, and microstructure of red-mud concrete. *Journal of the Korean Ceramic Society*, 57(2), 167-174.
- Verma NK, Meesala CR, Kumar S (2023). Developing an ANN prediction model for compressive strength of fly ash-based geopolymer concrete with experimental investigation. *Neural Computing and Appli*cations, 35, 10329–10345.
- Wang L, Chen L, Guo B, Tsang DCW, Huang L, Ok YS, Mechtcherine V (2020). Red mud-enhanced magnesium phosphate cement for remediation of Pb and As contaminated soil. *Journal of Hazardous Materials*, 400, 123317.
- Wang Y, Zhen Z (2024). Properties of red-mud-modified basic magnesium sulfate cement. *Materials*, 17(16), 4085.
- Yavuz D (2024). Freeze-thaw and drop-weight impact resistance of fiber-reinforced pervious concretes produced using recycled pervious concrete aggregate. Challenge Journal of Structural Mechanics, 10(4), 138-148.
- Yuan B, Yuan S, Straub C, Chen W (2020). Activation of binary binder containing fly ash and portland cement using red mud as alkali source and its application in controlled low-strength materials. *Journal of Materials in Civil Engineering*, 32(2), 04019356.
- Zhu J, Yue H, Ma L, Li Z, Bai R (2023). Study on hydration mechanism and environmental safety of thermal activated red mud-based cementitious materials. *Environmental Science and Pollution Research*, 30, 55905–55921.